Defect and Diffusion Forum
ISSN: 1662-9507, Vol. 434, pp 33-38
doi:10.4028/p-SHhhR7

Submitted: 2023-09-08
Revised: 2024-03-21
Accepted: 2024-03-22
Online: 2024-08-22

Early Detection of Bar-Shaped 1SSF before Expansion by PL Imaging

T. Morita[1,a*], Y. Matsushita[1,b], Y. Igarashi[1,c], K. Takano[1,d]

[1]ITES, 1-60, Kuribayashi-cho, Otsu-shi, Shiga, 520-2151, Japan

[a]takuya_morita@ites.co.jp, [b]yohsuke_matsushita@ites.co.jp, [c]yiga@ites.co.jp, [d]kazumi_takano@ites.co.jp

Keywords: Silicon carbide, photoluminescence, dislocation

Abstract. In this study, we investigated how bar-shaped 1SSF (Single Shockley-type stacking fault) in a chip of a SiC (Silicon Carbide) epitaxial wafer expanded with UV (ultraviolet) irradiation and observed it with PL (Photoluminescence) imaging and demonstrated early detection of bar-shaped 1SSF with an algorithm for automatic detection for the initial shape of bar-shaped 1SSF. Furthermore, we estimated that it was 83% how much UV irradiation time could be reduced.

Introduction

Electricity has been playing more and more important role in our society to the extent that we cannot go a day without hearing news about renewable energy and EVs. These industries require highly efficient semiconductors that can handle high voltages, high frequencies, which are not the range that silicon can cover due to its nature as a semiconductor, and research has been conducted on wide-bandgap semiconductors such as SiC and GaN (Gallium Nitride) as new possibilities for practical use [1].

Among the wide-gap semiconductors, SiC is a promising choice because of its dielectric breakdown strength, high thermal conductivity, and low anisotropy, and its manufacturing technology is becoming more proficient due to the previous intense research. Some defects in SiC have been technically cleared, such as Micropipe, while others are still in the process of being solved, such as BPD (basal plane dislocations) that is a line defect that lies on the (0001) plane of 4H-SiC. BPD in the drift layer of 4H-SiC devices can expand into 1SSF by REDG (recombination enhanced dislocation glide) when current flows, causing bipolar degradation that leads to forward voltage degradation. Although it is known that BPD stems from BPD originally in the substrate and during epitaxial growth converting BPD to TED (Threading Edge Dislocation) can suppress the propagation of BPDs to the epitaxial layer, it was found that TED-converted BPD nevertheless causes bipolar degradation at high current densities.

Therefore, EVC (Expansion-Visualization-Contraction) method was proposed in our previous report, which allows effective screen for malignant BPDs to support mass production of SiC in terms of time saving. The “Expansion” of this method intentionally utilizes the REDG mechanism by UV irradiation in wafer sorting [2]. It is well known from previous studies that 1SSFs gradually expand during forward conduction in SiC power devices, including bipolar operation, leading to an increase in on-resistance [3]. Isolating more detrimental defects through the detection of early shapes before complete expansion in PL image can contribute to the performance, yield, and reliability of SiC wafer fabrication. This motivates the development of early detection of 1SSFs which are likely to expand into bar-shaped, which is known to be more harmful because of its large area.

For early detection of 1SSFs which are likely to expand into bar-shaped, we investigated how bar-shaped 1SSF in a chip of a commercially available SiC epitaxial wafer expands with UV irradiation. It is well known that initial shapes of 1SSF are classified according to the combination of the direction of dislocation line and Burger’s vector [4] so we built an algorithm to detect 1SSFs based on the shape of 1SSFs in the early stage and derived the estimation of how much UV irradiation time could be reduced.

Experimental Procedures

To evaluate how early we can detect a 1SSF which is likely to expand into bar shaped 1SSF, we irradiated a chip with UV laser repetitively and observed it with PL each time to confirm the expansion of the bar-shaped 1SSF as show in Figure 1. And then we compared the difference between the earliest 1SSF detected in a series of PL images and the image that can be identified as a bar shape. Although it would be ideal if we could evaluate the limit of how early we can identify the shape of 1SSF which is likely to expand into bar-shape, it was hard at present because our existing equipment does not allow dynamic visualization of 1SSF expansion motion with UV irradiation. Thus, the limit of how early the 1SSF could be detected was estimated from the size of the initial shape based on the first image of the PL images which 1SSF was detected.

We used a chip of SiC epitaxial wafer with higher density of BPDs than typical epitaxial one for this experiment. The epitaxial layer with low carrier concentration 7.3×10^{15} had a thickness of 11.5 μ m and the crystal surface was the (0001) Si face at 4° off-angle toward $[11\bar{2}0]$. UV irradiation was performed with the device whose light source was Nd-YAG third harmonic with a wavelength of 355 nm. The sample chip was irradiated for 10 minutes repetitively at an irradiation intensity of 113.2 W/cm^2 with a diameter of 3 mm. PL observation was then performed with a PL imaging apparatus (PVX1000, ITES CO., LTD.) with a mercury lamp as excitation source with wavelength ranging from 285 nm to 350 nm and a 420 nm band-pass filter. PL image size was 2.66×2.66 mm^2 (1024×1024px).

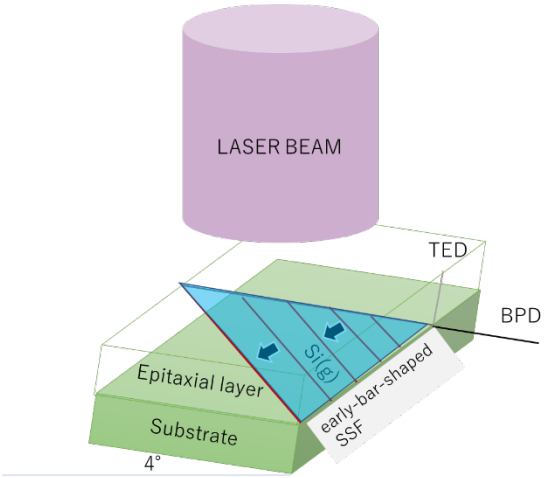

Fig. 1 Three-dimensional schematic diagram of the early shape of bar-shaped 1SSF and dislocations glide with UV irradiation.

Automatic Detection

To detect the position of early shape of bar-shaped 1SSF automatically, we applied the following procedure:

1. 1SSF candidate detection:

   A rectangular collection of bright spots that can be considered as 1SSF candidates is listed from the image and sorted within a certain range of width as shown in Figure 2 (a).

2. Half rhombic shapes detection from the upper and lower edge angle:

   i. Pick up the selected rectangular-shaped image, binarize it as shown in Figure 2 (b).

   ii. Count the bright spots horizontally in pixel units and add them together as shown in Figure 2 (b). Then divide the value array into two parts at the maximum value in the sense of splitting the half rhombic shape into upper and lower sides and determine the slope of the two sides by linear regression; if the coefficient of determination R^2 is high, the calculated

vertical angles are considered trusted. It is noted that R^2 is square of Pearson's product-moment correlation coefficient.

iii. If the calculated the upper edge angle and lower edge angle are within a certain range, it is assumed to be a half rhombic shape, and the initial shape of the defect is determined. That range is between ±10 of 30 degrees for the upper side and between ±10 of -30 degrees for the lower side.

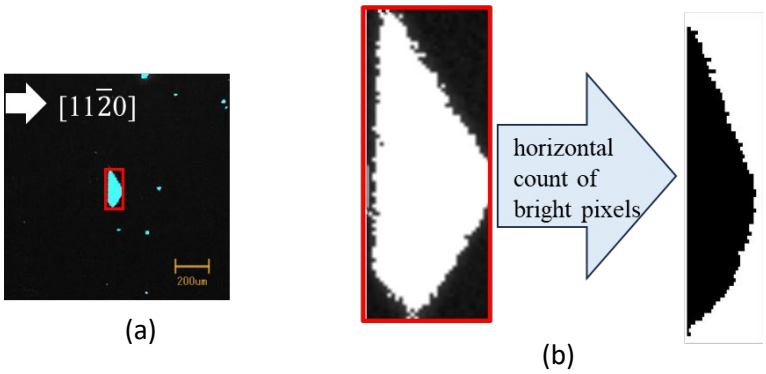

Fig. 2 Detection results of the original image
(a) A 1SSF candidate marked by red rectangle (b) The half rhombic shape marked in red rectangle is enlarged and binarized, and the result of horizontally counting the bright spots in the image in pixel units.

Results and Discussion

Repetitive UV Irradiation and PL Observation

Figure 3 (a) shows a series of PL images of 10-minute UV irradiations of the chip of SiC epitaxial wafer: after 10 minutes of UV irradiation, PL observations were made and repeated. The image after the first 10 minutes of irradiation shows a half rhombic shape that is the initial shape of the bar-shaped 1SSF measured at 94 μm, which was in the process of expanding and had not yet reached the epi-sub interface since the maximum width of 1SSF (W) was calculated from the following equation:

$$W = d/tan\theta \quad (1)$$

where d and θ represent the thickness of the epi-layer and the actual off-cut angle. The value of W was 164.5 μm. After further 10 minutes of irradiations, the same defect expanded diagonally and then vertically once it reached the surface. Figure 2 (b) shows the expansion mechanism from the combination of the direction of dislocation line and Burger's vector.

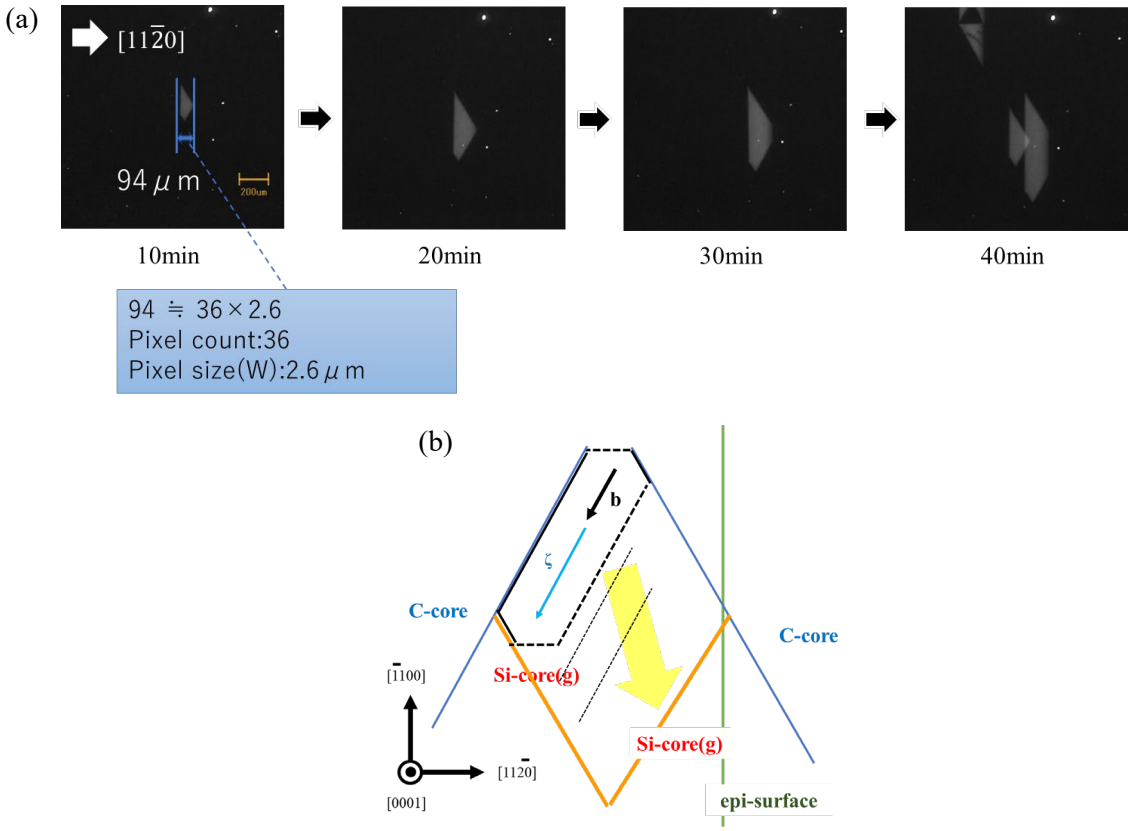

Fig. 3 (a) Transition of bar-shaped expansion in PL images after repetitive UV irradiation. Total UV irradiation time is below each image. (b) Schematic diagram of bar-shaped 1SSF expansion mechanism from the combination of the direction of dislocation line and Burger's vector.

The linear regression results of the upper and lower edge angles of the 10min-irradiation image in Figure 3(a) were shown in Table 1. The shape is considered identifiable because R^2 exceeded 0.9.

Table 1 Linear regression result of the upper and lower edge angles and coefficient of determination (R^2) of a half rhombic shape in the 10min-irradiation image in Figure 3(a).

	slope	angle	R^2
upper side	-0.62	-31.9	0.98
lower side	0.70	35.0	0.92

Estimates of How Much Time Could Be Reduced

To estimate how much time could be reduced, we compared the difference between the irradiation time when expanded to an obvious bar shape, which was determined from the fact that the 1SSF reached both edges of the epi-surface and the epi-sub-interface and expanded in the vertical direction, and that when expanded to an initial and detectable shape. The former was 30 minutes as shown in Figure 3. For the latter, since it was hard at present because our existing equipment does not allow dynamic visualization of 1SSF expansion motion with UV irradiation, we assumed that we could obtain the shape of 1SSF after half time of irradiation by reducing the size of the image by half, under the assumption that it expands at a constant rate.

The linear regression results of the upper and lower edge angles of the half size image and quarter size image were shown in Table 2 and those images were shown in Figure 4. In the half size image, the angles were close to those of the original image and R^2s still exceeded 0.9, while in the quarter size image, the R^2 of upper angle dropped to 0.77. The regression results of the quarter size image

showed that the R^2 was not so fit to correctly identify the defects because the image was too rough. This is why at the current image resolution, the result at half the irradiation time or 5 minutes, was found the limit of early detection. Thus, it turned out the irradiation time could be reduced from 30 minutes to 5 minutes, or by 83%.

Table 2 Linear regression result of the upper and lower edge angles and R^2 of a half rhombic shape in (a) the half size image, and (b) the quarter size image.

(a)

	slope	angle	R^2
upper side	-0.59	-30.6	0.96
lower side	0.79	38.3	0.9

(b)

	slope	angle	R^2
upper side	-0.56	-29.3	0.94
lower side	0.69	34.4	0.77

(a) (b)

Fig. 4 (a) the half size image and (b) quarter size image of a half rhombic shape

Summary and Issues

We repeated 10 minutes UV irradiations and PL to observe the process of expansion of 1SSF into bar shape. And we constructed an algorithm for the automatic detection of the initial shape of bar shape 1SSF. As a result, it was found UV irradiation time could be reduced by 83% thanks to the early detection of bar shape 1SSF. Since it was hard to know how little time initial shape of bar shape 1SSF showed up, we estimated the short UV irradiation time to expand to an initial and detectable shape was 5 minutes from the resolution of the image and the algorithm.

This study focused on the expansion process of a specific one of many bar-shaped 1SSFs of a specific chip of SiC epitaxial wafer. For practical use of the early detection of bar shape 1SSF, quantitative evaluation should be performed on larger areas such as other defects and those of other wafers.

Acknowledgements

METI Monozukuri R&D Support Grant Program for SMEs Grant Number JPJ005698

References

[1] B. J. Baliga, Fundamental of Power Semiconductor Devices (Springer, Berlin, 2008)

[2] Y. Igarashi, K. Takano, Y. Matsushita, C. Shibata, Defect and Diffusion Forum 425, 75 (2023).

[3] M.Skowronski and S.Ha, J. Appl. Phys. 99, 011101(2006).

[4] A. Iijima, I. Kamata, H. Tsuchida, J. Suda, and T. Kimoto, Philos. Mag. 97, 2736 (2017).